AN6017

Application note

VNHD7008AY and VNHD7012AY: minimizing electromagnetic emissions in practical circuit designs

Introduction

This application note is intended to provide guidelines for optimizing electromagnetic emissions in practical applications that use the DC motor driver VNHD7008AY or VNHD7012AY.

1 Case study: driving the steering motors

The document contains a comprehensive case study on a steering system and a simplified block diagram is illustrated in the figure below.

Figure 1. **Simplified block diagram of the steering system**

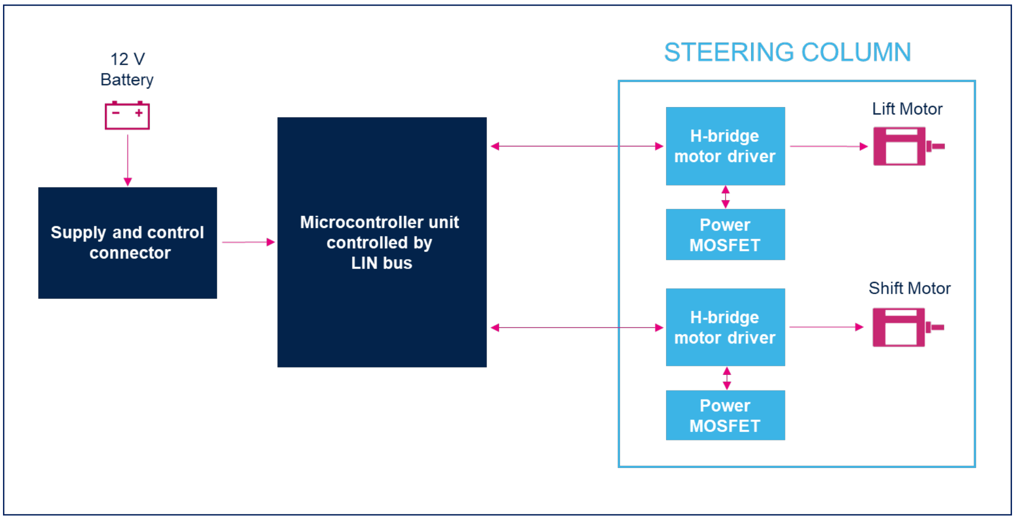

The analyzed application involves a motorized steering column that employs a two-motor system to control the steering position with precision and accuracy. This two-motor system enables the driver to make quick and accurate steering adjustments, especially during high-speed driving or emergency situations, thereby providing a high level of control and enhancing the overall safety of the vehicle.

The DC lift and shift motors are driven by the half-bridge (H-bridge) motor driver VNHD7008AY or VNHD7012AY coupled to the low-voltage (LV) power MOSFET STL76DN4LF7AG or STL64DN4F7AG in a double island configuration, as external low-side (LS) switch.

The VNHD7008AY and VNHD7012AY are AEC-Q100 automotive qualified dual DC motor drivers with fully integrated protections and monitoring functions, designed with STMicroelectronics' VIPower M0-7 technology and housed in a PowerSSO 36 package. The STL76DN4LF7AG and STL64DN4F7AG are both 40 V power MOSFETs, AEC-Q101 automotive qualified, designed with STMicroelectronics' STripFET F7 technology and housed in a dual island PowerFLAT 5x6 package.

The motor driving system communicates with the external components through two connectors. The input connector contains the battery line harness and the LIN (local interconnect network) control signal, while the output connector is wired to the terminals of the motor loads. Both motors can be driven in clockwise and counterclockwise modes at a frequency of 20 kHz and a pulsed power supply with a duty cycle of 85%.

2 Electromagnetic emission measurements

To analyze electromagnetic emissions within a specific frequency band, a rod monopole antenna set-up is utilized in accordance with the international standard CISPR 25. The measurements are conducted in an anechoic chamber, as shown in the block diagram in the figure below.

Figure 2. Block diagram of the electromagnetic emission test set-up

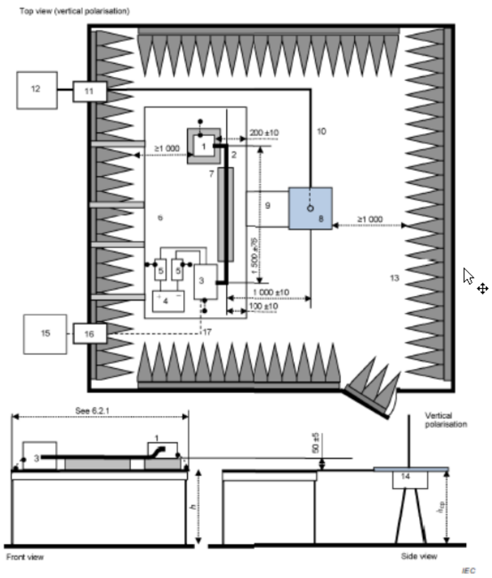

In the above figure, the legend is as below:

1. EUT (equipment under test), grounded locally if required in test plan.
2. Test harness.
3. Load simulator.
4. Power supply (location optional).
5. AN (artificial network).
6. Reference ground plane (bonded to shielded enclosure).
7. Low relative permittivity support ($\varepsilon_r \leq 1.4$).
8. Rod antenna with counterpoise (dimensions: 600 mm by 600 mm typical)
   h = (900 ± 100) mm
   h_{cp} = h + (+10 / -20) mm.
9. Grounding connection (full width bond between counterpoise and reference ground plane).
10. High-quality coaxial cable, for example, double-shielded (50 Ω).
11. Bulkhead connector.
12. Measuring instrument.
13. RF absorber material.
14. Antenna matching unit (the preferred location is below the counterpoise; if above the counterpoise then the base of the antenna rod shall be at the height of the reference ground plane).
15. Stimulation and monitoring system.
16. Fiber optic feed through.
17. Optical fibers.

Electromagnetic interference (EMI) is measured using an emission test receiver located outside the chamber. The receiver's parameters are set according to the CISPR 25 standard, as reported in table below.

Table 1. **Emission parameters of the test receiver (CISPR 25 standard)**

Service/band	Frequency [MHz]	Peak detection			Quasi-peak detection			Average detection		
		BW at -6 dB	Max. step size	Min. meas. time	BW at -6 dB	Max. step size	Min. meas. time	BW at -6 dB	Max. step size	Min. meas. time
BROADCAST LW MW SW FM TV band I TV band III DAB III TV band IV/V DTT DAB L band SDARS	0.15 to 0.30 0.53 to 1.8 5.9 to 6.2	9 kHz	5 kHz	50 ms	9 kHz	5 kHz	1 s	9 kHz	5 kHz	50 ms
	76 to 108 41 to 88 174 to 230 171 to2 45 468 to 944	120 kHz	50 kHz	5 ms	120 kHz	50 kHz	1 s	120 kHz	50 kHz	5 ms
	470 to 770 1447 to 1494 2320 to 2345	120 kHz	50 kHz	5 ms	Does not apply	Does not apply	Does not apply	120 kHz	50 kHz	5 ms

In the above table, the legend is as below:
LW = long wave
MW = medium wave
SW = short wave
FM = frequency modulation
TV band = television band
DAB = digital audio broadcasting
DTT = digital terrestrial television
SDARS = satellite digital audio radio service.

3 Experimental results

The figure below is a picture of the lab test set-up.

Figure 3. **Picture of the lab test set-up**

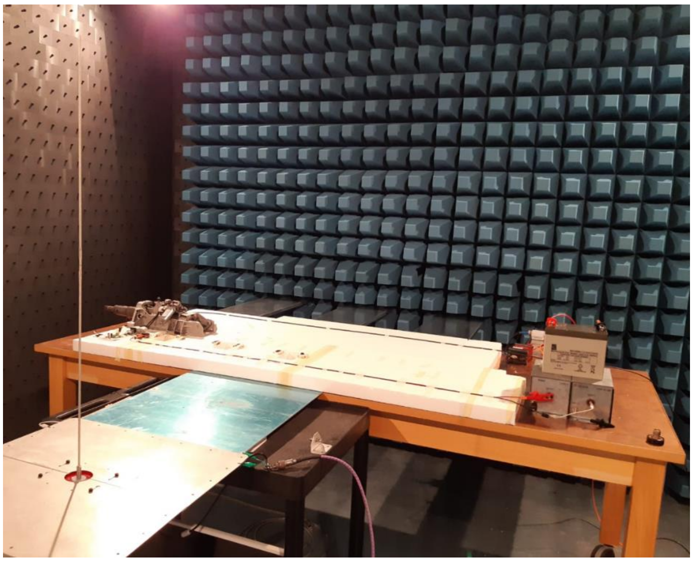

In the set-up depicted in the figure above, the rod monopole antenna is equipped with a preamplifier and its ground plane must be electrically connected to the table ground.

To stabilize the line impedance, two LISNs (line impedance stabilizing network) are placed on both the battery line and ground return path of the board. A 12 V battery supply is utilized to eliminate any noise caused by electronic power suppliers. Additionally, a correction factor (antenna factor) is applied to the measured emissions to account for the conversion coefficient between the voltage read at the antenna output and the corresponding electric field intensity.

The emissions are captured through both peak and average detectors on the original application board, where the steering column is not connected to the ground.

Figure 4. **Measured emission waveforms with the original board**

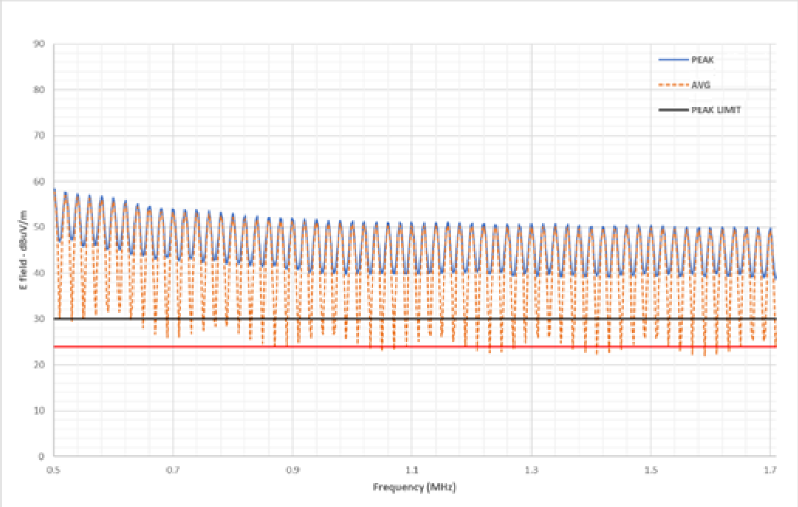

High levels of emissions are detected in the AM (amplitude modulation) band, including LW, MW, and SW, particularly in the frequency range between 0.5 MHz and 1.7 MHz, exceeding the limit specifications.

4 Guidelines for EMI optimization

4.1 Ground connection

The first guideline, which was implemented and verified in the case study, involves directly connecting the steering column body to the system ground. The average and peak emission graphs with this modification are shown in the figure below.

Figure 5. Measured emission waveforms with ground connection

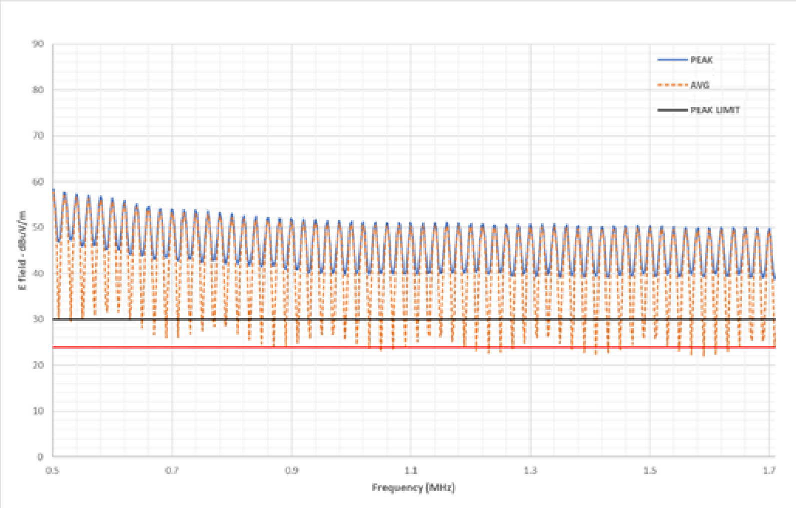

The measured waveforms demonstrate that connecting the steering column body to the ground results in a visible improvement in EMC performance for both peak and average measurements.

The analysis performed on the system revealed that the emissions are primarily caused by two factors:

1. Harmonics of the PWM (pulse-width modulation) signal.
2. Hard and asymmetrical slopes of the rising and falling edges.

The VNHD7008AY and VNHD7012AY do not have embedded circuitry to reshape the switching slopes, and filtering the input noise is challenging due to the high current flowing level in the battery line.

As a conclusion, high saturation current inductor filters would be required, which impact the final cost of the application platform.

4.2 Slowing down the switching edges

An additional guideline to reduce emissions in the 0.5 MHz - 1.7 MHz band is to slow down the switching edges. The following steps can be taken to achieve this goal:

1. Add an additional gate-drain capacitor to increase the total gate-drain capacitance and slow down the switching phase of the LS power MOSFET.
2. Increase the MOSFET gate resistance and introduce an asymmetrical gate driving circuitry to balance the rising and falling edges.
3. Modify the capacitance value of the input filter.

4.2.1 Adding a gate-drain capacitor

The addition of an extra gate-drain capacitor, without modifying the value of the gate resistor of the LS external power MOSFETs, leads to an average reduction in emissions as follows:

- about 10 dBµV/m in the frequency range of 0.5 MHz ~ 0.8 MHz
- about 20 dBµV/m between 0.8 MHz and 1.7 MHz.

where dBµV/m indicates decibels voltage level referenced to 1 microvolt per meter.

The improvement is not affected by whether or not the steering column body is grounded. However, including the ground connection in the solution can help to reduce electromagnetic interference and improve the overall performance of the system. Therefore, this solution is preferable.

To prevent the sudden shutdown of the system, a value of 470 pF or lower is recommended for the extra gate-drain capacitor. This is because a higher value can trigger the V_{DS} (drain-source voltage) protection of the half bridge IC (integrated circuit). Although higher values (up to 560 pF) can work well, it is important to consider the tolerance of the capacitance values (which can reach 10%) and the differences observed at hot (125 °C) and cold (-40 °C) temperatures. To account for these factors, a safe margin should be ensured.

The figure below shows the emissions with the extra gate-drain capacitor and steering column connected to ground, which is the best result that could be obtained with this circuit modification.

Figure 6. **Measured emission waveforms with ground connection and extra gate-drain capacitor**

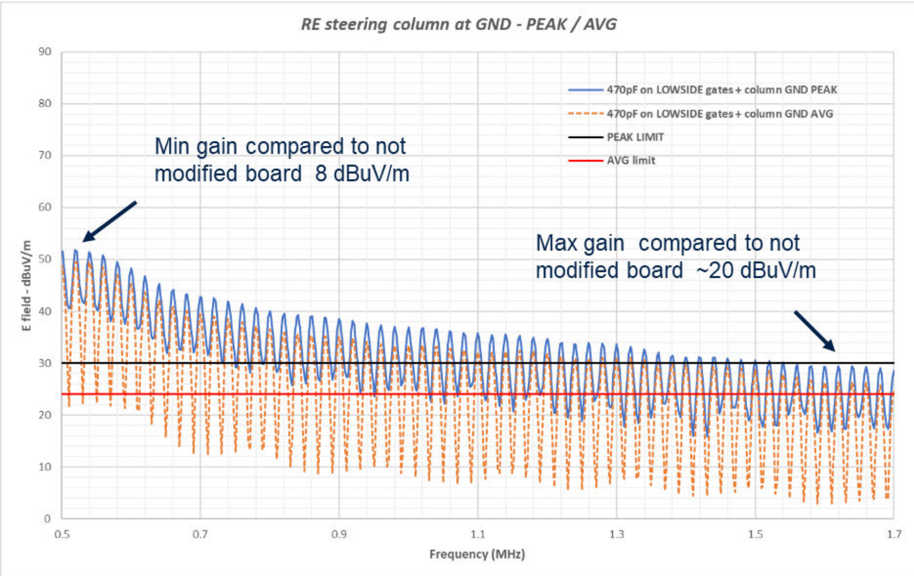

4.2.2 Increasing the gate resistance with an asymmetrical gate driving

These circuit optimizations are simultaneously implemented, by increasing the resistance from the output of the half bridge motor drivers to the gate of the LS MOSFETs and considering the circuit shown below.

Figure 7. Proposed circuit for asymmetrical gate driving

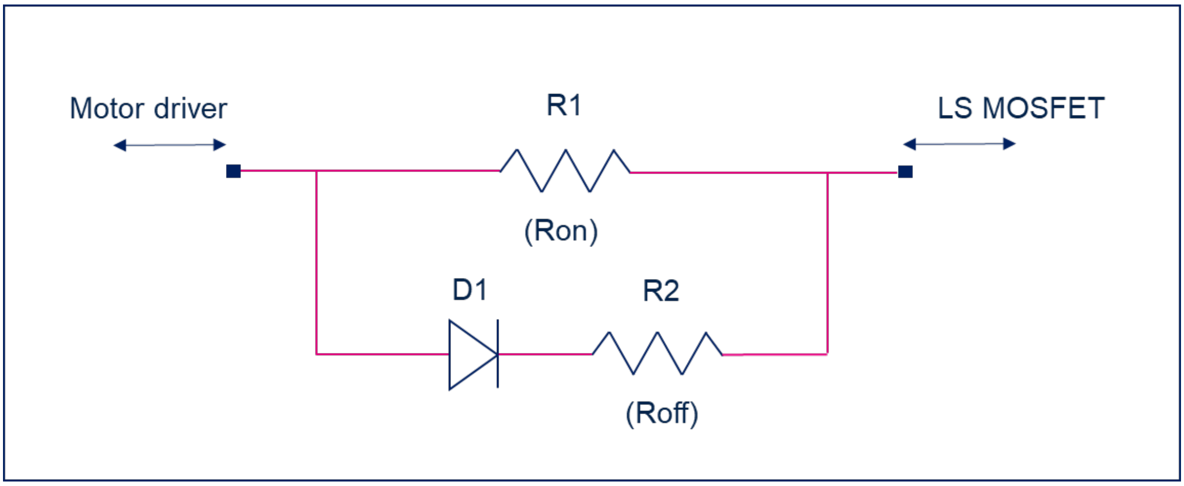

To reduce the electromagnetic emissions, the gate resistance (R1) can be increased by:

- changing the R1 value from 470 Ω to 1 kΩ.

Asymmetrical gate driving is achieved by adding a diode (D1) with a resistance (R2) set to 470 Ω.

The combination of the two solutions - increasing the gate resistance and introducing asymmetrical gate driving - along with increasing the gate-drain capacitance results in more balanced switching waveforms with smoother rising and falling edges on the motor's terminals.

This effect can be observed in the figure below, showing the emission waveforms with the steering column body connected to the ground.

Figure 8. Measured emission waveforms with ground connection and circuit improvements

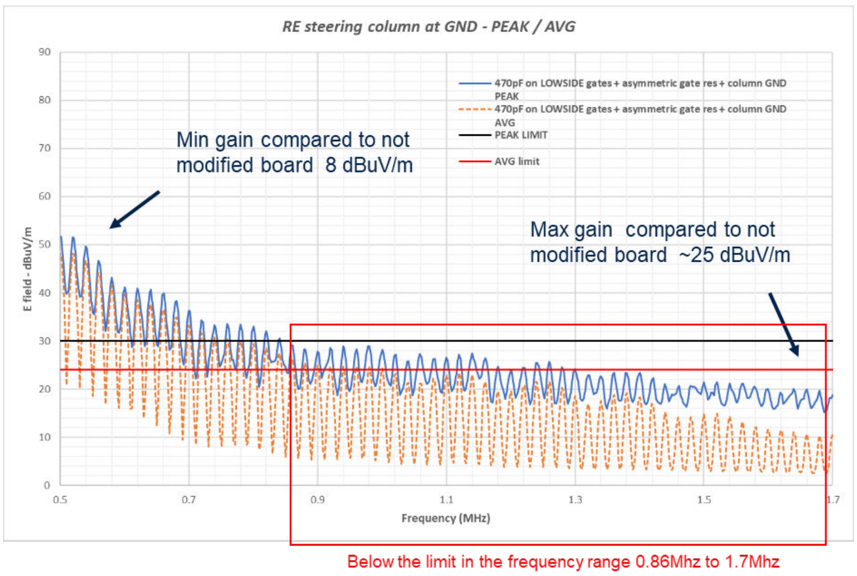

As a result, the proposed solution allows for emission levels to be maintained below the normative limits of the CISPR 25 standard from 0.9 MHz up to 1.7 MHz.

To provide a clearer explanation of the effect of the asymmetric gate driver, it is useful to consider some test measurements conducted on an application board loaded with a dummy resistive-inductive (R-L) load:

- 2 Ω resistor with 13 μH inductor.

When a 470 Ω gate resistor is mounted on the LS MOSFET gates, the falling switching edges are much quicker (about 170 ns) compared to the rising ones (about 800 ns).

By introducing the asymmetric gate driver shown in Figure 7. Proposed circuit for asymmetrical gate driving with the following values:

- R1 = 1000 Ω
- R2 = 470 Ω

The falling and rising switching shapes are more balanced. The relevant waveforms are shown in the figure below, where the red curve is the gate-source voltage (V_{GS}) of the MOSFETs, the blue curve is the PWM (pulse width modulation) control signal and the yellow curve is the voltage on the load.

Figure 9. Measured switching waveforms with asymmetrical gate driving

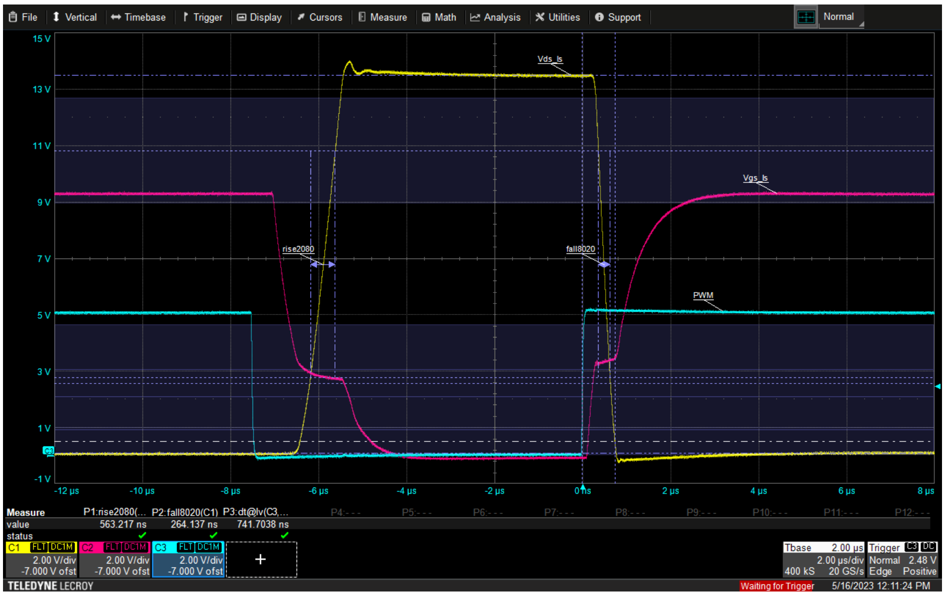

The rising time is reduced due to the lower gate resistance resulting from the parallel of the two resistances R1 and R2 (equal to about 320 Ω), while the fall time is increased up to 270 ns.

In conclusion, the combination of more balanced rise and fall switching times, along with slowing down of the switching times (resulting in a reduction of associated harmonics), leads to an overall improvement in emission rate.

4.2.3 Modifying the input filter capacitance

It is recommended to add an extra capacitor immediately after the input supply connector and before the filtering inductor (1 µH) to obtain a further reduction of emissions, especially in the lowest part of the frequency range.

The cumulative effects of all suggested modifications are shown in the figure below, displaying both peak and average measured spectrum.

Figure 10. Measured emission waveforms with all suggested circuit modifications

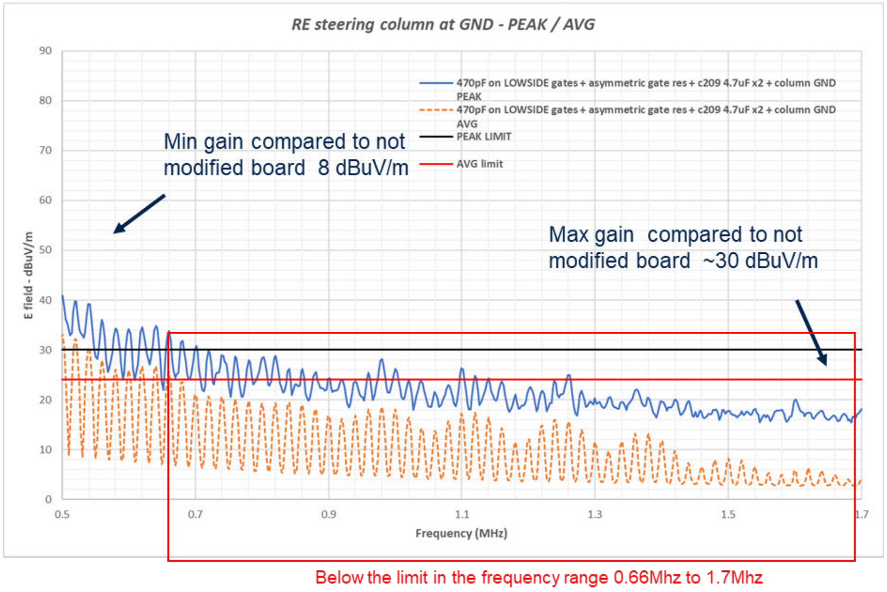

There is still a small frequency interval where emissions are above the standard specification limits. These values could be reduced with an additional input filter, which can increase the performance from a minimum of 10 dBµV/m up to 30 dBµV/m maximum with an impact on the final cost of the application.

5 Conclusions

The following figure concludes by comparing the emission spectrum in the initial case (blue line) and suggested solution (yellow line), summarizing and highlighting the global improvement obtained.

Figure 11. Measured emission comparison between the initial case and suggested solutions

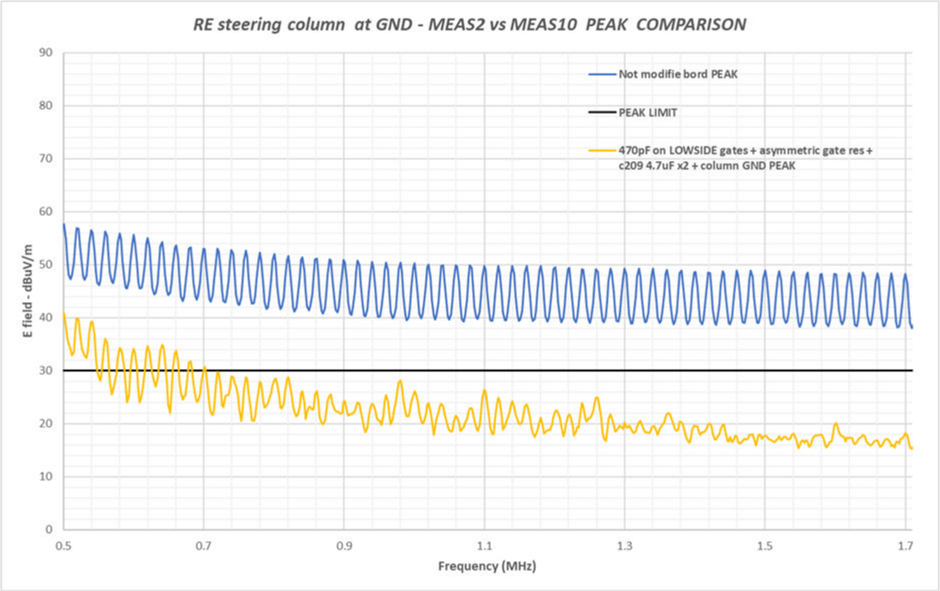

All suggested application modifications can effectively reduce the emission rate of a DC motor control system, making it compliant with the CISPR-25 standard specification limits in the 0.5 MHz - 1.7 MHz bandwidth.

The mean reduction of peak emissions obtained with the different solutions implemented in sequence is summarized in the table below.

Table 2. Mean reductions of peak emissions with all suggested circuit modifications

Conditions	Peak emission reduction [dBµV/m]	
	Low freq. (0.5 MHz – 0.8 MHz)	High freq. (0.8 MHz – 1.7 MHz)
Ground connection	2 dBµV/m	2 dBµV/m
Extra gate-drain capacitor	10 dBµV/m	20 dBµV/m
Increase gate resistance with asymmetrical driving	20 dBµV/m	25 dBµV/m
Extra filtering capacitor	25 dBµV/m	30 dBµV/m

Revision history

Table 3. **Document revision history**

Date	Revision	Changes
22-Sep-2023	1	First release.

Contents

1 Case study: driving the steering motors . . . 2
2 Electromagnetic emission measurements . . . 3
3 Experimental results . . . 5
4 Guidelines for EMI optimization . . . 6
4.1 Ground connection . . . 6
4.2 Slowing down the switching edges . . . 6
4.2.1 Adding a gate-drain capacitor . . . 6
4.2.2 Increasing the gate resistance with an asymmetrical gate driving . . . 8
4.2.3 Modifying the input filter capacitance . . . 10
5 Conclusions . . . 11
Revision history . . . 12
List of tables . . . 14
List of figures . . . 15

List of tables

Table 1. Emission parameters of the test receiver (CISPR 25 standard) 4
Table 2. Mean reductions of peak emissions with all suggested circuit modifications 11
Table 3. Document revision history 12

List of figures

Figure 1. Simplified block diagram of the steering system 2
Figure 2. Block diagram of the electromagnetic emission test set-up 3
Figure 3. Picture of the lab test set-up 5
Figure 4. Measured emission waveforms with the original board 5
Figure 5. Measured emission waveforms with ground connection 6
Figure 6. Measured emission waveforms with ground connection and extra gate-drain capacitor 7
Figure 7. Proposed circuit for asymmetrical gate driving 8
Figure 8. Measured emission waveforms with ground connection and circuit improvements 8
Figure 9. Measured switching waveforms with asymmetrical gate driving 9
Figure 10. Measured emission waveforms with all suggested circuit modifications 10
Figure 11. Measured emission comparison between the initial case and suggested solutions 11